

Fermi-surface evolution and pseudogap symmetry in n -type cuprate superconductors

Y. Zhou,^{1,2} H. Q. Lin,² and C. D. Gong¹

¹*National Laboratory of Solid State Microstructure, Department of Physics, Nanjing University, Nanjing 210093, People's Republic of China*

²*Department of Physics and the Institute of Theoretical Physics, Chinese University of Hong Kong, Hong Kong, People's Republic of China*

(Received 12 February 2008; published 27 March 2008)

Based on a doping dependent t - t' - t'' - J Hamiltonian, the pseudogap and the structure of the Fermi surface are studied as a function of electron doping. No extra adjustable parameter is introduced and no gap associated order parameter is preassumed. The evolution from the small electron pocket centered at $(\pi, 0)$ to the large holelike Fermi surface centered at (π, π) upon increasing the doping level is revealed. A clear flat region near the hot spot is formed, which accounts for the opening of the pseudogap. Both the position and the magnitude of this pseudogap are consistent with the experiments. The influence of the pseudogap on the measured superconducting gap and difference between the electron- and hole-doped cuprates are also discussed.

DOI: [10.1103/PhysRevB.77.092510](https://doi.org/10.1103/PhysRevB.77.092510)

PACS number(s): 74.25.Jb, 71.18.+y, 71.27.+a, 74.20.Mn

For the past 20 years, the quasiparticle (QP) dispersion, Fermi surface (FS), and symmetry of the superconducting energy gap and the pseudogap, including their doping evolution in hole-doped cuprates, had been well studied.¹ Recently, many experiments on $\text{Nd}_{2-x}\text{Ce}_x\text{CuO}_{4\pm\delta}$ (Refs. 2–4) and $\text{Pr}_{1-x}\text{LaCe}_x\text{CuO}_{4-y}$ (Ref. 5) show that the behavior of physical properties in electron-doped cuprates is quite different from that in the hole-doped cuprates, for example, the doping evolution of the FS and the symmetry of the superconducting (SC) energy gap and pseudogap. The high-resolution angle-resolved photoemission spectroscopy (ARPES) experiments reveal that the FS of the electron-doped case evolves from a small electron pocket centered around $(\pi, 0)$ at low doping level to a large-three-pieced FS centered at (π, π) near the optimal doping level.³ On the other hand, the symmetry of the SC energy gap and pseudogap is quite controversial. Previous ARPES experiments,⁶ the specific heat,⁷ and phase-sensitive scanning superconducting quantum interference device measurement⁸ indicated that it was of d -wave symmetry. However, the possibility of containing s -wave components and other symmetry, deviated from the standard $d_{x^2-y^2}$ form, i.e., the *nonmonotonic* d -wave symmetry, was also proposed based on experimental evidence.^{5,9–11} In addition, the relationship between the pseudogap and the SC energy gap is also controversial.

Theoretically, the evolution of the FS has been extensively studied.^{12–15} The small electron packet centered around $(\pi, 0)$ in the underdoped case was predicted by the t - t' - U model.¹² However, its application to the high electron doping case seems inconsistent with experiments; the large FS is still unformed even at 0.12 doping level, as shown in Fig. 4 of Ref. 12. This situation can be improved by introducing an adjustable effective Hubbard constant U_{eff} in the extended t - t' - t'' - U model.¹³ This phenomenological U_{eff} , whose origin is not clearly clarified, is not necessary and is thought to be too small to stabilize the antiferromagnetic order as discussed in detail by Yuan *et al.*¹⁴ In the Kotliar-Ruckenstein slave-boson approximation scheme, Yuan *et al.* showed a full evolution of the FS¹⁴ by choosing an interme-

diate U and found that the intensity near the $(\pi/2, \pi/2)$ region is weakened for optimal doping and enhanced for underdoping, as compared to experiments. The evolution of the FS with doping was also qualitatively obtained by applying the slave-boson mean-field method to the t - J model.¹⁵ Nevertheless, they did not address the pseudogap symmetry issue and their approach is more suitable for the underdoped case. Numerically, the QP dispersion had been calculated by the exact diagonalization (ED) technique,¹⁶ and the evolution of the FS from electron pockets to large FS was also predicted¹⁷ on the 20 site lattice. The limitations of the small lattice size and doping concentration prevent these methods from further application. The small electron pockets and QP dispersion in slightly electron-doped cuprates were studied by using the variational Monte Carlo (VMC) method,¹⁸ but not full FS evolution. Though much progress had been made, the nature of the pseudogap remains open. Its momentum and doping dependence is still a puzzling issue.

In this Brief Report, the evolution of the FS and the pseudogap symmetry will be studied in the framework of the extended t - J model. An effective doping dependent Hamiltonian is obtained under the slave-fermion approximation. Except the values of t and J obtained from the experiments, no arbitrary parameter is introduced, and no gap order is preassumed. The evolution of small electron pocket centered at $(\pi, 0)$ to the large holelike FS centered at (π, π) is found, and the turning point is estimated at doping concentration $x=0.1$. A flat region around the hot spot is formed. The largest gap is opened at the hot spot and slightly decreases when deviating from the hot spot. The existence of the pseudogap will change the measured SC energy. We attribute the difference between the electron- and hole-doped cases to the different locations of the hot spots. In this Brief Report, the theoretical results obtained are in good agreement with recent experiments.^{3–5}

We start from the t - t' - t'' - J model, which is an extension of the usual t - J model, and apply the electron-hole transformation.^{17–20} Using the slave-fermion representation, a doping dependent effective spin-polaron Hamiltonian takes the form²¹

TABLE I. The ED results of the spin-spin correlation function and corresponding renormalization factor in an 18-site cluster with different electron dopings.

x	$\langle ij \rangle_1$	$\langle ij \rangle_2$	$\langle ij \rangle_3$	I_1	I_2	I_3
0.0	-0.347	0.217	0.200	-0.097	0.817	0.8
0.056	-0.28	0.156	0.138	-0.03	0.406	0.388
0.111	-0.233	0.089	0.045	0.017	0.339	0.295
0.167	-0.181	0.045	0.021	0.069	0.295	0.271
0.222	-0.158	0.016	0.0	0.092	0.266	0.25

$$H_{eff} = \sum_q \omega_q b_q^\dagger b_q + \sum_k \epsilon_k h_k^\dagger h_k + \sum_{kq} M_{kq} h_k^\dagger h_{k-q} b_q, \quad (1)$$

where h and b are the spinless fermion and spin-1/2 spinon operators, respectively. Here, $\omega_q = 2\sqrt{E_q^2 - \Delta_q^2}$ with $E_q = \tilde{J}[1 + (1 - \alpha)\gamma_q]$ and $\Delta_q = \alpha\tilde{J}\gamma_q$, with $\alpha = 0.802$ being the ratio of the condensed bosons to the total bosons on a 128×128 lattice, large enough to eliminate the size effect. $\tilde{J} = J(1 - \delta)^2$, where δ defines electron doping level. The bare dispersion is $\epsilon_k = 4I_1 t \gamma_k + 4I_2 t' \lambda_k + 4I_3 t'' \eta_k$, with $\gamma_k = \frac{1}{2}(\cos k_x + \cos k_y)$, $\lambda_k = \cos k_x \cos k_y$, and $\eta_k = \frac{1}{2}(\cos 2k_x + \cos 2k_y)$. Because of Fermi statistics, the hopping constants (t, t', t'') each have an extra minus sign in comparison with the hole-doping case. All results presented below are based on the following parameters: $J = 0.4$, $t = -1$ (~ 0.4 eV), $t' = 0.3$, and $t'' = -0.2$.²² The renormalization factors I_i ($i = 1, 2, 3$) are the correlation function for nearest neighbor (nn), next-nn, second-next-nn, respectively. It takes the form $I_i = \frac{1}{4} + \langle \tilde{S}_i \cdot \tilde{S}_j \rangle + \frac{1}{2}(\langle S_i^z \rangle + \langle S_j^z \rangle)$. The spinon-fermion coupling function M_{kq} is

$$M_{kq} = \frac{4\sqrt{\alpha}}{\sqrt{N}} [u_q(t\gamma_{k-q} + t'\lambda_{k-q} + t''\eta_{k-q}) + v_q(t\gamma_k + t'\lambda_k + t''\eta_k)], \quad (2)$$

where u_q and v_q are the usual Bogoliubov transformation parameters. Both the bare dispersion and the spinon-fermion coupling are doping dependent, and so is the effective Hamiltonian. As noted before, no extra parameter is introduced and no gap associated order parameter is preassumed in the H_{eff} .

The ED method is performed to calculate the spin-spin correlation $\langle \tilde{S}_i \cdot \tilde{S}_j \rangle$, and the corresponding renormalization factors with different doping levels are shown in Table I. Compared to the case of hole-doped cuprates,²¹ the absolute values of spin-spin correlations all more slowly decrease. It is obvious that all effective hopping terms are much depressed due to the presence of those renormalization factors, especially for the nn hopping term due to incoherent scattering induced in the electron hopping between two neighboring sites, while there is no such effect produced in the electron hopping between two next-nn and second-next-nn sites. We can estimate the value of I_i for arbitrary doping levels from Table I by fitting those data. For example, they are -0.06 , 0.46 , and 0.45 , respectively, at $x = 1/64$; correspondingly, the effective hopping constants ($I_i t^i$) are -0.06 , 0.14 , and -0.09 , well consistent with the results obtained by the

VMC method.¹⁸ The self-consistent Born approximation is used to evaluate the QP dispersion based on the doping dependent H_{eff} .

The evolution of the FS structure upon electron doping is illustrated in Fig. 1 for four densities. A remarkable cross-over from the small FS pocket at low doping to a large FS near the optimal doping is found. At low doping level, for example, $x = 0.04$ in Fig. 1(a), the electron pockets are formed around $(\pi, 0)$.³ These electron pockets provide clear evidence of electron-hole asymmetry, since the hole arc centers around $(\pi/2, \pi/2)$ in the hole-doping case.²³ The shape of the FS gradually changes with further doping. For example, in Fig. 1(b), $x = 0.1$, the FS tends to be larger centered at (π, π) . When $x = 0.13$, the strongest spectral intensity is found around $(\pi, 0)$, a weak but observable intensity appears around $(\pi/2, \pi/2)$, and a negligible intensity can be found between these two regions. Thus, the so-called peak-dim-hump FS structure is formed as experimentally discovered.⁴ At the optimal doping level, as shown in Fig. 1(d), the strongest intensity appears near $(\pi, 0)$ and $(\pi/2, \pi/2)$; thus, a large-three-pieced FS from $(\pi, 0.33\pi)$ to around $(\pi/2, \pi/2)$ is formed.³ Along the diagonal direction, the FS centers at about $(0.46\pi, 0.46\pi)$, which is also confirmed by the ARPES experiments.³ Another important feature is that the so-called hot spot locates near the negligible dim region, i.e., around $(0.7\pi, 0.3\pi)$, which slightly deviates from the experimental data $(0.65\pi, 0.3\pi)$.³ The doping evolution of the FS structure can be interpreted in terms of the structure of QP dispersion,

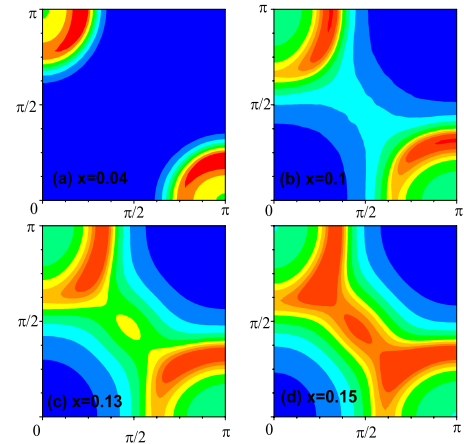


FIG. 1. (Color online) Fermi-surface maps in electron-doped case for different electron doping x . (a) $x = 0.04$, (b) $x = 0.1$, (c) $x = 0.13$, and (d) $x = 0.15$.

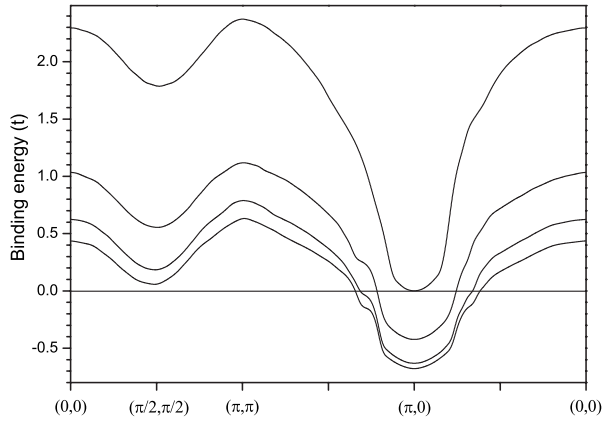


FIG. 2. The QP dispersion with different doping levels. The electron concentrations, from above to below at $(\pi, 0)$, are 0, 0.04, 0.1, and 0.15. The Fermi energy is fixed at zero.

as shown in Fig. 2. For the low doping case, the QP energy around the $(\pi/2, \pi/2)$ region is much higher above the Fermi energy, and the doped electrons only enter into the $(\pi, 0)$ region, which leads to the small electron pocket. The $(\pi/2, \pi/2)$ region gradually approaches to the Fermi energy upon doping density increases. Correspondingly, the doped electron begins to enter in this region, and the weak intensity emerges near the $(\pi/2, \pi/2)$ region. Around the optimal doping, the $(\pi/2, \pi/2)$ region is closer to the FS, and parts of the doped electrons enter into this region, which leads to the large-three-pieced FS. It should be pointed out that the chemical potential can still be defined in the conventional way due to the broadened QP peak near the hot spot, as shown in Fig. 3(a).³ The spectral function of the quasiparticle is well peaked near the region of $(\pi, 0)$ and $(\pi/2, \pi/2)$, especially near the antinodal region. However, the peak of the quasiparticle spectral function near the hot spot is strongly broadened.^{3,4} Our theoretical results are consistent with the ARPES observations.^{3,4}

Next, we show the momentum dependence of the pseudogap by taking the case of $x=0.15$ as an example. Fig-

ure 3(a) is the evolution of the spectral function along the $(\pi, 0)$ to (π, π) direction. A clear flat region of QP dispersion is formed, as shown in Fig. 3(b). For example, $k_x = \pi$, is located around 0.25π , slightly away from the experimentally observed 0.3π .^{3,5} This position gradually moves toward the hot spot when k_x is deviating away from π . Similar behavior is found along k_x for given k_y near the electron pocket. Thus, the center of this flat region does not locate at $(\pi, 0)$ anymore, but at $(0.75\pi, 0.23\pi)$, a position nearby the hot spot, and the related energy gap is opened. The distance below the FS of this flat region is about $0.15t$ (60 meV) of the same order compared to the experimental data with 100 meV.³ It should be pointed out that the distance of the flat QP dispersion reaches its maximum at the hot spot and slightly decreases deviating from it. Similar to the hole-doped cuprates, the position of this flat region is just the same as where the pseudogap appears.^{3,4} Along the diagonal direction, the QP peak is always above the Fermi energy, and no anomaly is found (not shown). Thus, the pseudogap is only opened near the hot-spot region, in comparison to the opening related pseudogap near the antinode in the hole-doped case.^{21,24} On the other hand, the order of magnitude of the pseudogap is larger than that of the experimental SC energy gap (~ 3 meV) in electron-doped cuprates, which is thought to be the evidence that the pseudogap and SC gap come from different origins.^{3,5,25,26} As a comparison, they are in the same order in the hole-doped cuprates.

The opening pseudogap will dramatically influence the measured symmetry of the SC energy gap. The experimental measurements show that the best fitting of the SC energy gap is nonmonotonic d -wave with the form of $\Delta(\theta) = \Delta_0[(1+B)\cos(2\theta) - B\cos(6\theta)]$, i.e., a significant shift of largest value away from $(\pi, 0)$ toward $(\pi/2, \pi/2)$ is found.^{5,11} This nonmonotonic behavior can be realized as the substantial influence comes from the pseudogap to SC gap. Near the hot spot, the magnitude of the SC energy gap is enhanced due to the opening of the pseudogap in this region with its maximum value appearing at the hot spot, where the largest pseudogap is opened. Beyond this region, the measured SC energy gap keeps unchanged due to disappearance

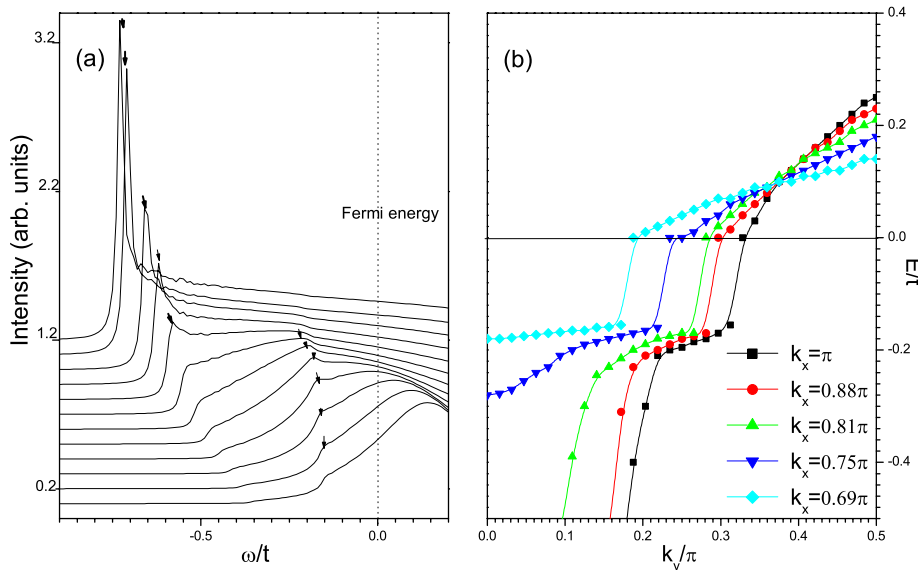


FIG. 3. (Color online) (a) Spectral function along the $(\pi, 0)$ to (π, π) direction. The arrows indicate the peak of spectral function and are guides for the eyes. From top to bottom, k_y increases from 0 to 0.406π . Dotted line shows the Fermi energy. (b) Evolution of QP dispersion in k_y direction with different k_x .

of the pseudogap, which means that the SC gap is still simple d -wave symmetry. Such an opinion is supported by the recent ARPES measurements on the SC gap and pseudogap.²⁷ This can interpret the previous controversy on the symmetry of the SC gap in the electron-doped cuprates, such as a dirty d -wave in specific heat measurement,⁷ d -wave pairing with impurity scattering in penetration depth measurement,²⁸ and even the possible s -wave symmetry near the antinodes.¹⁰ In fact, even in the hole-doped cuprates, the symmetry of the SC gap is also nonmonotonic d -wave^{27,29} due to the same reason, though this nonmonotonic is much weaker and often confused with the simple d -wave symmetry.

We notice that within our theoretical framework, the only difference between the electron-doped and hole-doped cases is the different signs of hopping terms, so the question of why the pseudogap shows distinct behavior is naturally put forward. As revealed by Eq. (2), the spinon-fermion coupling function is largest for the momentum transfer $Q=(\pi, \pi)$, which connects the electronic states at the intersection of antiferromagnetic Brillouin-zone boundary and the FS, so the largest gap is expected to locate near the hot spot where the spin fluctuations most strongly couple to the electrons on the FS.^{4,5} In the electron-doped case, the hot spot moves from $(\pi, 0)$ to $(\pi/2, \pi/2)$ upon increasing the doping level, and it locates at $(0.7\pi, 0.3\pi)$ for $x=0.15$, the intermediate position between the $(\pi, 0)$ and $(0, 0)$. In contrast, this posi-

tion is close to the point $(\pi, 0)$ in the hole-doped case (also see Fig. 1 of Ref. 5) and almost unchanged from the underdoped case to the overdoped case. Hence, a simple- d wave-like form is enough to describe the symmetry of the SC gap.

In conclusion, based on a doping dependent Hamiltonian, the pseudogap and the evolution of the FS were studied. The crossover from small electron FS pockets centered at $(\pi, 0)$ at low doping level ($\leq x=0.1$) to large holelike FS centered at (π, π) at high doping level is described satisfactorily in our theoretical framework, and it is well consistent with experiments. A flat region is formed around the hot spot, which accounts for the opening of the pseudogap. This pseudogap will dramatically change the measured symmetry of the SC gap. We attribute the difference between the electron-doped and hole-doped cuprates to the different positions of the hot spot. It should be stressed that no arbitrary parameter is introduced and no gap associated order parameter is preassumed in our work.

We acknowledge discussion with J. X. Li. This work was financially supported by HKRGC (Grant No. 402205), the National Nature Science Foundation of China (Grant No. 90503014), and the State Key Program for Basic Researches of China (Grant No. 2006CB921802). C.D.G. would also like to thank the 973 Project (2006CB601002).

¹A. Damascelli *et al.*, Rev. Mod. Phys. **75**, 473 (2003).

²D. M. King *et al.*, Phys. Rev. Lett. **70**, 3159 (1993).

³N. P. Armitage *et al.*, Phys. Rev. Lett. **87**, 147003 (2001); N. P. Armitage *et al.*, *ibid.* **88**, 257001 (2002).

⁴H. Matsui *et al.*, Phys. Rev. Lett. **94**, 047005 (2005).

⁵H. Matsui *et al.*, Phys. Rev. Lett. **95**, 017003 (2005).

⁶N. P. Armitage *et al.*, Phys. Rev. Lett. **86**, 1126 (2001); T. Sato *et al.*, Science **291**, 1517 (2001).

⁷H. Balci *et al.*, Phys. Rev. B **66**, 174510 (2002).

⁸C. C. Tsuei and J. R. Kirtley, Phys. Rev. Lett. **85**, 182 (2000).

⁹B. Stadlober *et al.*, Phys. Rev. Lett. **74**, 4911 (1995); C.-T. Chen *et al.*, *ibid.* **88**, 227002 (2002).

¹⁰L. Shan *et al.*, Phys. Rev. B **72**, 144506 (2005).

¹¹G. B. Blumberg *et al.*, Phys. Rev. Lett. **88**, 107002 (2002).

¹²H. Kusunose and T. M. Rice, Phys. Rev. Lett. **91**, 186407 (2003).

¹³C. Kusko *et al.*, Phys. Rev. B **66**, 140513(R) (2002).

¹⁴Qingshan Yuan, F. Yuan, and C. S. Ting, Phys. Rev. B **72**, 054504 (2005).

¹⁵Qingshan Yuan *et al.*, Phys. Rev. B **69**, 214523 (2004).

¹⁶R. J. Gooding, K. J. E. Vos, and P. W. Leung, Phys. Rev. B **50**,

12866 (1994).

¹⁷T. Tohyama and S. Maekawa, Phys. Rev. B **64**, 212505 (2001); T. Tohyama, *ibid.* **70**, 174517 (2004).

¹⁸T. K. Lee, C. M. Ho, and N. Nagaosa, Phys. Rev. Lett. **90**, 067001 (2003).

¹⁹J. X. Li, J. Zhang, and J. Luo, Phys. Rev. B **68**, 224503 (2003).

²⁰T. Tohyama and S. Maekawa, Phys. Rev. B **49**, 3596 (1994).

²¹W. G. Yin, C. D. Gong, and P. W. Leung, Phys. Rev. Lett. **81**, 2534 (1998); W. G. Yin and C. D. Gong, Phys. Rev. B **56**, 2843 (1997).

²²O. K. Andersen *et al.*, Phys. Rev. B **49**, 4145 (1994).

²³M. R. Norman *et al.*, Nature (London) **392**, 157 (1998).

²⁴D. S. Marshall *et al.*, Phys. Rev. Lett. **76**, 4841 (1996).

²⁵L. Alff *et al.*, Nature (London) **422**, 698 (2003).

²⁶B. Lake *et al.*, Nature (London) **400**, 43 (1999); B. Lake *et al.*, Science **291**, 1759 (2001).

²⁷T. Kondo *et al.*, Phys. Rev. Lett. **98**, 267004 (2007); K. Terashima *et al.*, *ibid.* **99**, 017003 (2007).

²⁸A. Snezhko *et al.*, Phys. Rev. Lett. **92**, 157005 (2004).

²⁹K. McElroy *et al.*, Nature (London) **422**, 592 (2003); J. Mesot *et al.*, Phys. Rev. Lett. **83**, 840 (1999).